

International Journal of Modern Physics: Conference Series
 © The Authors

Quark and Glue Components of the Proton Spin from Lattice Calculation*

Keh-Fei Liu[†]

*Department of Physics and Astronomy, University of Kentucky
 Lexington, KY 40506 USA[‡]*

The status of lattice calculations of the quark spin, the quark orbital angular momentum, the glue angular momentum and glue spin in the nucleon is summarized. The quark spin calculation is recently carried out from the anomalous Ward identity with chiral fermions and is found to be small mainly due to the large negative anomaly term which is believed to be the source of the 'proton spin crisis'. We also present the first calculation of the glue spin at finite nucleon momenta.

Keywords: quark spin, glue spin, proton spin

PACS numbers: 12.38.Gc, 11.40.Ha, 12.38.-t, 14.20.Dh

1. Introduction

Apportioning the spin of the nucleon among its constituents of quarks and glue is one of the most challenging issues in QCD both experimentally and theoretically.

Since the contribution from the quark spin is found to be small ($\sim 25\%$ of the total proton spin) from the global analysis of deep inelastic scattering data ¹, it is expected that the remainder should come from glue spin and the orbital angular momenta of quarks and glue. The quark spin contribution from u , d and s has been studied on the lattice ^{2,3} since 1995 with quenched approximation or with heavy dynamical fermions ⁴. Recently, it has been carried out with light dynamical fermions ^{5,6,7,8} for the strange quark. We will report the calculation of both the connected insertion (CI) and disconnected insertion (DI) contributions to quark spin from u , d , s and c using anomalous Ward identity from the overlap fermion ¹¹.

As for the quark orbital angular momenta, lattice calculations have been carried out for the connected insertions (CI) ^{12,13,14,15,16,17,18,19}. They are obtained by subtracting the quark spin contributions from those of the quark angular momenta.

*Plenary talk presented at SPIN2014, the 21st International Symposium on Spin Physics.

[†]On behalf of χ QCD Collaboration

[‡]liu@pa.uky.edu

2 *K.F. Liu*

It has been shown that the contributions from u and d quarks almost cancel each other. Thus for connected insertion, quark orbital angular momenta turn out to be small in the quenched calculation^{12,14} and nearly zero in dynamical fermion calculations^{15,16,17,18,19}. On the other hand, gluon helicity distribution $\Delta G(x)/G(x)$ from COMPASS, STAR, HERMES and PHENIX experiments is found to be close to zero^{20,21,22,23,24}. A global fit²⁵ with the inclusion of the polarized deep inelastic scattering (DIS) data from COMPASS²⁶ and the 2009 data from RHIC²⁵, gives a glue contribution $\int_{0.05}^{0.2} \Delta g(x) dx = 0.1 \pm_{0.07}^{0.06}$ to the total proton spin of $1/2\hbar$ with a sizable uncertainty. Most recent analysis²⁷ of high-statistics 2009 STAR²⁸ and PHENIX²⁹ data show an evidence of non-zero glue helicity in the proton. For $Q^2 = 10 \text{ GeV}^2$, they found the gluon helicity distribution $\Delta g(x, Q^2)$ positive and away from zero in the momentum fraction range $0.05 \leq x \leq 0.2$. However, the result presented in⁷ has very large uncertainty in the small x -region. Moreover, it is argued based on analysis of single-spin asymmetry in unpolarized lepton scattering from a transversely polarized nucleon that the glue orbital angular momentum is absent³⁰. Given that DIS experiments and quenched lattice calculation thus far reveal that only $\sim 25\%$ of the proton spin comes from the quark spin, lattice calculations of the orbital angular momenta show that the connected insertion (CI) parts have negligible contributions, and gluon helicity from the latest global analysis²⁷ is $\sim 40\%$ albeit with large error, there are still missing components in the proton spin. In this context, it is dubbed a ‘Dark Spin’ conundrum^{31,32}.

In this talk, I shall present a complete decomposition of the nucleon spin in terms of the quark spin, the quark orbital angular momentum, and the glue angular momentum in a quenched lattice calculation. I will then summarize the lattice effort in calculating the strange quark spin in dynamical fermions and present a result of the total quark spin from a lattice calculation employing the anomalous Ward identity and, finally, I will show a preliminary first calculation of the glue spin at finite nucleon momenta.

2. Formalism

It is shown by X. Ji³³ that there is a gauge-invariant separation of the proton spin operator into the quark spin, quark orbital angular momentum, and glue angular momentum operators

$$\vec{J}_{\text{QCD}} = \vec{J}_q + \vec{J}_g = \frac{1}{2} \vec{\Sigma}_q + \vec{L}_q + \vec{J}_g, \quad (1)$$

where the quark and glue angular momentum operators are defined from the symmetric energy-momentum tensor

$$J_{q,g}^i = \frac{1}{2} \epsilon^{ijk} \int d^3x (\mathcal{T}_{q,g}^{0k} x^j - \mathcal{T}_{q,g}^{0j} x^k), \quad (2)$$

with the explicit expression

$$\vec{J}_q = \frac{1}{2}\vec{\Sigma}_q + \vec{L}_q = \int d^3x \left[\frac{1}{2} \bar{\psi} \vec{\gamma} \gamma^5 \psi + \psi^\dagger \{ \vec{x} \times (i\vec{D}) \} \psi \right], \quad (3)$$

for the quark angular momentum which is the sum of quark spin and orbital angular momentum, and each of which is gauge invariant. The glue angular momentum

$$\vec{J}_g = \int d^3x \left[\vec{x} \times (\vec{E} \times \vec{B}) \right], \quad (4)$$

is also gauge invariant. However, since it is derived from the symmetric energy-momentum tensor in the Belinfante form, it cannot be further divided into the glue spin and orbital angular momentum gauge invariantly.

Since the quark orbital angular momentum and glue angular momentum operators in Eqs. (3) and (4) depends on the radial vector \vec{r} , a straight-forward application of the lattice calculation is complicated by the periodic condition of the lattice, and may lead to wrong results³⁴. Hence, instead of calculating J_q and J_g directly, we shall calculate them from the energy-momentum form factors in the nucleon.

The Euclidean energy-momentum operators for the quark and glue are

$$\mathcal{T}_{\{4i\}q}^{(E)} = (-1) \frac{i}{4} \sum_f \bar{\psi}_f \left[\gamma_4 \vec{D}_i + \gamma_i \vec{D}_4 - \gamma_4 \overleftarrow{D}_i - \gamma_i \overleftarrow{D}_4 \right] \psi_f, \quad (5)$$

$$\mathcal{T}_{\{4i\}g}^{(E)} = (+i) \left[-\frac{1}{2} \sum_{k=1}^3 2 \text{Tr}^{\text{color}} [G_{4k} G_{ki} + G_{ik} G_{k4}] \right]. \quad (6)$$

where we use the Pauli-Sakurai representation for the gamma matrices and the covariant derivative is the point-split lattice operator involving the gauge link U_μ . For the gauge field tensor $G_{\mu\nu}$, we use the overlap fermion Dirac operator. The connection between $G_{\mu\nu}$ and the overlap Dirac operator has been derived^{35,36}

$$\text{Tr}_s [\sigma_{\mu\nu} D_{\text{ov}}(x, x)] = c_T a^2 G_{\mu\nu}(x) + \mathcal{O}(a^3), \quad (7)$$

where Tr_s is the trace over spin. $c_T = 0.11157$ is the proportional constant at the continuum limit for the parameter $\kappa = 0.19$ in the Wilson kernel of the overlap operator which is used in this work. The overlap Dirac operator $D_{\text{ov}}(x, y)$ is exponentially local and the gauge field $G_{\mu\nu}$ as defined in Eq. (7) is chirally smoothed so that it admits good signals for the glue momentum and angular momentum in the lattice calculation³².

The form factors for the quark and glue energy-momentum tensor are defined as

$$\begin{aligned} \langle p', s' | \mathcal{T}_{\{4i\}q,g}^{(E)} | p, s \rangle = & \left(\frac{1}{2} \right) \bar{u}^{(E)}(p', s') \left[T_1(-q^2) (\gamma_4 \bar{p}_i + \gamma_i \bar{p}_4) \right. \\ & \left. - \frac{1}{2m} T_2(-q^2) (\bar{p}_4 \sigma_{i\alpha} q_\alpha + \bar{p}_i \sigma_{4\alpha} q_\alpha) - \frac{i}{m} T_3(-q^2) q_4 q_i \right] u^{(E)}(p, s). \end{aligned} \quad (8)$$

4 *K.F. Liu*

where the normalization conditions for the nucleon spinors are

$$\bar{u}^{(E)}(p, s) u^{(E)}(p, s) = 1, \quad \sum_s u^{(E)}(p, s) \bar{u}^{(E)}(p, s) = \frac{\not{p} + m}{2m}, \quad (9)$$

2.1. Sum rules and renormalization

The momentum and angular momentum fractions of the quark and glue depend on the renormalization scale and scheme individually, but their sums do not because the total momentum and angular momentum of the nucleon are conserved. We shall use the sum rules as the renormalization conditions on the lattice.

Substituting the energy-momentum tensor matrix elements in Eq. (8) to the matrix elements which define the angular momentum in Eq. (2) and a similar equation for the momentum, it is shown³³ that

$$J_{q,g} = \frac{1}{2} Z_{q,g}^L [T_1(0) + T_2(0)]_{q,g}, \quad (10)$$

$$\langle x \rangle_{q,g} = Z_{q,g}^L T_1(0)_{q,g}. \quad (11)$$

where $Z_{q,g}^L$ is the renormalization constant for the lattice quark/glue operator. $\langle x \rangle_{q,g}$ is the second moment of the unpolarized parton distribution function which is the momentum fraction carried by the quark or glue inside a nucleon. The other form factor, $T_2(0)_{q,g}$, can be interpreted as the anomalous gravitomagnetic moment in analogy to the anomalous magnetic moment, $F_2(0)$ ^{37,38}.

Since momentum is always conserved and the nucleon has a total spin of $\frac{1}{2}$, we write the momentum and angular momentum sum rules using Eqs. (1), (10) and (11), as

$$\langle x \rangle_q + \langle x \rangle_g = Z_q^L T_1(0)_q + Z_g^L T_1(0)_g = 1, \quad (12)$$

$$J_q + J_g = \frac{1}{2} \left\{ Z_q^L [T_1(0) + T_2(0)]_q + Z_g^L [T_1(0) + T_2(0)]_g \right\} = \frac{1}{2}. \quad (13)$$

It is interesting to note that from Eqs. (12) and (13), one obtains that the sum of the $T_2(0)$'s for the quarks and glue is zero, i.e.

$$Z_q^L T_2(0)_q + Z_g^L T_2(0)_g = 0. \quad (14)$$

We used these sum rules and the raw lattice results to obtain the lattice renormalization constants Z_q^L and Z_g^L and then use perturbation³⁹ to calculate the quark-gluon mixing and renormalization in order to match to the \overline{MS} scheme at 2 GeV which preserves the sum rules.

2.2. Results of a lattice calculation with quenched approximation

Before we present the lattice results, we should point out that the three-point functions for quarks which are needed to extract the form factors in Eq. (8) have two topologically distinct contributions in the path-integral diagrams: one from

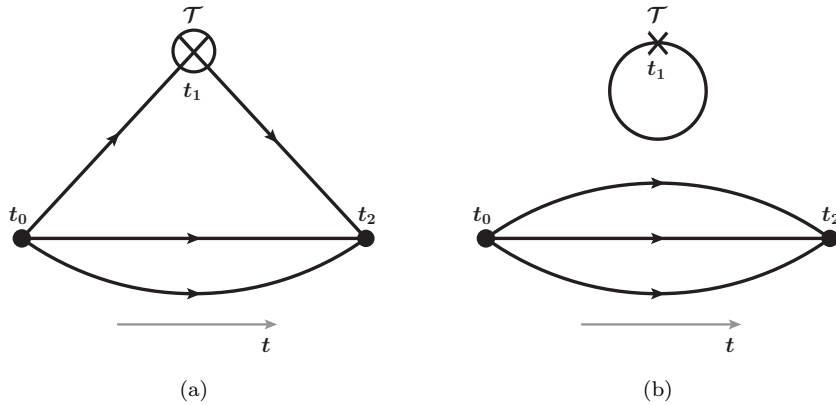


Fig. 1. Quark line diagrams of the three-point function with current insertion in the Euclidean path integral formalism. (a) Connected insertions (CI), and (b) disconnected insertions (DI).

connected insertions (CI) and the other from disconnected insertions (DI) ^{40,41,42,43} (See Figs. 1). They arise in different Wick contractions, and it needs to be stressed that they are not Feynman diagrams in perturbation theory. In the case of CI, quark/anti-quark fields from the operator are contracted with the quark/anti-quark fields of the proton interpolating fields. It represent the valence and the higher Fock space contributions from the Z -graphs. In the case of DI, the quark/anti-quark fields from the operator contract themselves to form a current loop, which represents the vacuum polarization of the disconnected sea quarks.

It should be pointed out that, although the quarks lines in the loop and the nucleon propagator appear to be ‘disconnected’ in Fig 1(b), they are in fact correlated through the gauge background fluctuation. In practice, the uncorrelated part of the loop and the proton propagator is subtracted. The disconnected insertion (DI) refers to the fact that the quark lines are disconnected. For the nucleon, the up and down quarks contribute to both CI and DI, while the strange and charm quarks contribute to the DI only.

A quenched lattice calculation on has been carried out with 3 valence quark masses and extrapolated to the physical pion mass where the numerical details of the calculation are given ³². We shall present the results in the following table.

For the unrenormalized lattice results, we find that $[T_2^u(0) + T_2^d(0)]$ (CI) is positive and $T_2^g(0)$ negative, so that the total sum including the small $[T_2^u(0) + T_2^d(0) + T_2^s(0)]$ (DI) can be naturally constrained to be zero (See Eq. (14)) with the lattice normalization constants $Z_q^L = 1.05$ and $Z_g^L = 1.05$ close to unity. As discussed in Sec. 2.1, the vanishing of the total $T_2(0)$ is the consequence of momentum and angular momentum conservation.

The flavor-singlet g_A^0 which is the quark spin contribution to the nucleon has been calculated before on the same lattice ². We can subtract it from the total quark angular momentum fraction $2J$ to obtain the orbital angular momentum fraction

6 *K.F. Liu*

 Table 1. Renormalized results in \overline{MS} scheme at $\mu = 2$ GeV.

	CI(u)	CI(d)	CI(u+d)	DI(u/d)	DI(s)	Glue
$\langle \boldsymbol{x} \rangle$	0.413(38)	0.150(19)	0.565(43)	0.038(7)	0.024(6)	0.334(55)
$\boldsymbol{T}_2(\mathbf{0})$	0.286(108)	-0.220(77)	0.062(21)	-0.002(2)	-0.001(3)	-0.056(51)
$\mathbf{2J}$	0.700(123)	-0.069(79)	0.628(49)	0.036(7)	0.023(7)	0.278(75)
\boldsymbol{g}_A	0.91(11)	-0.30(12)	0.62(9)	-0.12(1)	-0.12(1)	–
$\mathbf{2L}$	-0.21(16)	0.23(15)	0.01(10)	0.16(1)	0.14(1)	–

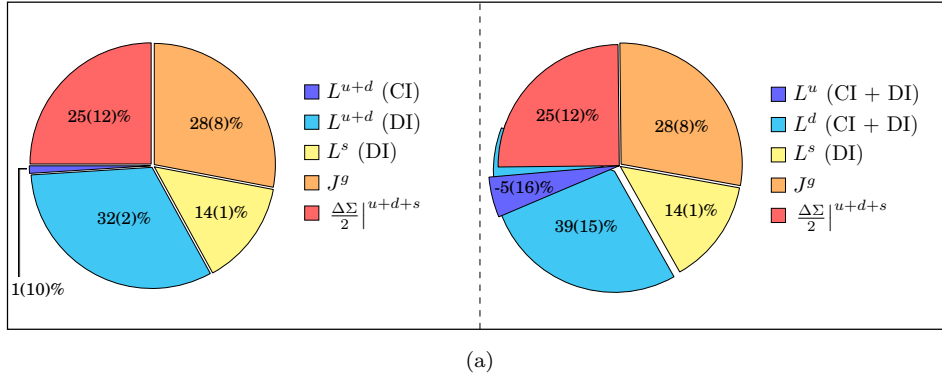


Fig. 2. Pie charts for the quark spin, quark orbital angular momentum and gluon angular momentum contributions to the proton spin. The left panel show the quark contributions separately for CI and DI, and the right panel shows the quark contributions for each flavor with CI and DI summed together for u and d quarks.

$2L$ for the quarks. As we see in Table 1, the orbital angular momentum fractions $2L$ for the u and d quarks in the CI have different signs and they add up to zero, i.e. 0.01(10). This is the same pattern which has been seen with dynamical fermion configurations with light quarks which was pointed out in Sec. 1. The large $2L$ for the u/d and s quarks in the DI is due to the fact that g_A^0 in the DI is large and negative, i.e. $-0.12(1)$ for each of the three flavors. All together, the quark orbital angular momentum constitutes a fraction of 0.47(13) of the nucleon spin. The majority of it comes from the DI. The quark spin fraction of the nucleon spin is 0.25(12) and the glue angular momentum contributes a fraction of 0.28(8). We show the quark spin, the quark orbital angular momentum and the glue angular momentum in the pie chart in Fig. 2. The left panel shows the combination of u and d contributions to the orbital angular momentum from the CI and DI separately while the right panel shows the combined (CI and DI) contributions to the orbital angular momentum from the u and d quarks.

Since this calculation is based on a quenched approximation which is known to contain large uncontrolled systematic errors, it is essential to repeat this calculation with dynamical fermions of light quarks and large physical volume.

3. Quark spin from anomalous Ward identity

Attempts have been made to tackle the proton spin decomposition with light dynamical fermions configurations. There have been a number of calculations of the strange quark spin ^{5,6,7,8} which found the strange quark spin Δs to be in the range from -0.02 to -0.03 which is several times smaller than that from a global fit of DIS and semi-inclusive DIS (SIDIS) which gives $\Delta s \approx -0.11$ ¹. The large negative contribution from the strange quark is confirmed by a recent analysis ⁹ of the world data on inclusive deep inelastic scattering data including COMPASS 2010 proton data on the spin asymmetries and the precise JLab CLAS data on the proton and deuteron spin structure functions which gives $\Delta s + \Delta \bar{s} = -0.106 \pm 0.023$ ¹⁰.

Such a discrepancy between the global fit of experiments and the lattice calculation of the quark spin from the axial-vector current has raised a concern that the renormalization constant for the flavor-singlet axial-vector current could be substantially different from that of the flavor-octet ^{44,45} at the lattice cutoff of ~ 2 GeV. The latter is commonly used for the lattice calculations of the flavor-singlet axial-vector current for the quark spin. To alleviate this concern, we use the anomalous Ward identity (AWI) to calculate the quark spin ¹¹. The anomalous Ward identity includes a triangle anomaly in the divergence of the flavor-singlet axial-vector current

$$\partial^\mu A_\mu^0 = 2 \sum_{f=1}^{N_f} m_f \bar{q}_f i \gamma_5 q_f + i N_f 2q, \quad (15)$$

where q is the local topological charge operator and is equal to $\frac{1}{16\pi^2} G_{\mu\nu}^\alpha \tilde{G}^{\alpha\mu\nu}$ in the continuum. We put this identity between the nucleon states and calculate the matrix element on the right-hand side with a momentum transfer \vec{q} and take the $|\vec{q}| \rightarrow 0$ limit

$$\langle p' s | A_\mu | p s \rangle s_\mu = \lim_{\vec{q} \rightarrow 0} \frac{i |\vec{s}|}{\vec{q} \cdot \vec{s}} \langle p', s | 2 \sum_{f=1}^{N_f} m_f \bar{q}_f i \gamma_5 q_f + 2i N_f q | p, s \rangle. \quad (16)$$

Lattice theory has finally accommodated vector chiral symmetry, the lack of which has hampered the development of chiral fermions on the lattice for many years. It is shown that when the lattice massless Dirac operator satisfies the Gingparg-Wilson relation $\gamma_5 D + D \gamma_5 = a D \gamma_5 D$ with the overlap fermion being an explicit example ⁴⁶, the modified chiral transformation leaves the action invariant and gives rise to a chiral Jacobian factor $J = e^{-2i\alpha \text{Tr} \gamma_5 (1 - \frac{1}{2} a D)}$ from the fermion determinant ⁴⁷. The index theorem ⁴⁸ shows that this Jacobian factor carries the correct chiral anomaly. It is shown further that the local version of the overlap Dirac operator gives the topological charge density operator in the continuum ⁴⁹, i.e.

$$\text{Tr} \gamma_5 (1 - \frac{1}{2} a D_{ov}(x, x)) = \frac{1}{16\pi^2} G_{\mu\nu}^\alpha \tilde{G}^{\alpha\mu\nu}(x) + \mathcal{O}(a) \quad (17)$$

Therefore, Eq. (15) is exact on the lattice for the overlap fermion which gives the correct anomalous Ward identity at the continuum limit. Instead of calculating the

8 *K.F. Liu*

matrix element of the axial-vector current derived from the Noether procedure^{50,48}, we shall calculate it from the r.h.s. of the AWI in Eq. (15) through the form factors defined in Eq. (16).

In the lattice calculation with the overlap fermion, we note that the renormalization constant of the pseudoscalar density cancels that of the renormalization of the quark mass, i.e. $Z_m Z_P = 1$ for the chiral fermion. Also, the topological charge density, when calculated with the overlap Dirac operator as in the l.h.s of Eq. (17) is renormalized – its integral over the lattice volume is an integer satisfying the Atiyah-Singer theorem. Thus, when the matrix elements on the right-hand side of Eq. (16) are calculated with the overlap fermion and its Dirac operator, the flavor-singlet axial-vector current is automatically renormalized on the lattice non-perturbatively *à la* anomalous Ward identity (AWI).

Besides the fact that AWI admits non-perturbative renormalization on the lattice, the pseudoscalar density in DI and the topological density represent the low-frequency and high-frequency parts of the divergence of the axial-vector quark loop respectively. It is learned that on the $24^3 \times 64$ lattice, a mere 20 pairs of the overlap low eigenmodes would saturate more than 90% of the pseudoscalar loop in configurations with zero modes⁵¹. On the other hand, it is well-known that the contribution to the triangle anomaly comes mainly from the cut-off of the regulator. Therefore, the topological charge density represents the high-frequency contribution of the axial-vector loop, albeit in a local form (the overlap operator is exponentially local). Since the pseudoscalar density is totally dominated by the low modes, we expect that the low-mode averaging (LMA) approach should be adequate for this term. To the extent that the signal for the anomaly term is good, we should be able to calculate the flavor-singlet g_A with the AWI. Both the overlap fermion for the quark loop and the overlap operator for the topological charge density are crucial in this approach.

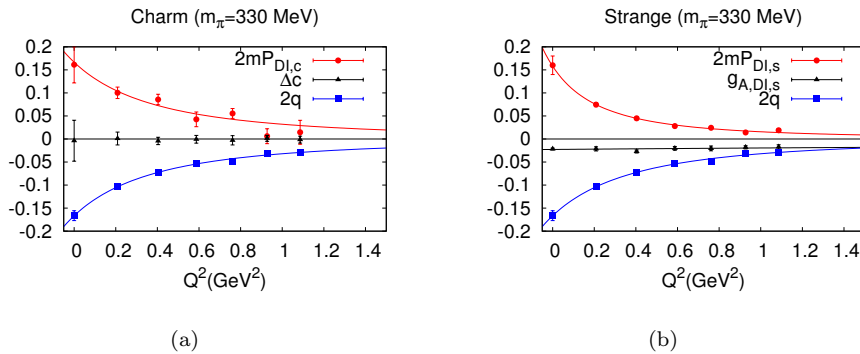


Fig. 3. (a) The charm pseudoscalar and topological density contributions to the proton spin as a function of Q^2 . (b) The same as in (a) for the strange.

With the approach described above, we have seen good signals on the $24^3 \times 64$ lattice with the sea quark mass corresponding to a pion mass at 330 MeV ¹¹. We first show the results for the charm quark which contribute only in the DI. The pseudoscalar density term and the topological charge density term are plotted in Fig. 3(a) as a function of Q^2 . We see that the pseudoscalar term is large and positive, while the topological charge term is large and negative. When they are added together (black triangles in the figure), it is consistent with zero for the whole range of Q^2 . When extrapolated to $Q^2 = 0$, the charm gives zero contribution to the proton spin within error due to the cancellation between the pseudoscalar term and the topological term. It is shown ⁵² that the leading term in the heavy quark expansion of the quark loop of the pseudoscalar density, i.e. $2mP$ is the topological charge $\frac{2i}{16\pi^2} \text{tr}_c G_{\mu\nu} \tilde{G}_{\mu\nu}$, but with a negative sign. Thus, one expects that there is no contribution to the quark spin from heavy quarks to leading order. It appears that the charm quark is heavy enough so that the $\mathcal{O}(1/m^2)$ correction is small. We take this as a cross check of the validity of our numerical estimate of the DI calculation of the quark loop as well as the anomaly contribution.

The contributions from the strange are also calculated and shown in Fig. 3(b). The $2mP$ contribution is slightly smaller than that of $2q$ and results in a net small negative value for the sum of $2mp$ and $2q$ at finite Q^2 . After a dipole fit, we obtain $\Delta s = -0.026(5)$ at $m_\pi = 330$ MeV. Here, Δs denotes the contributions for both s and \bar{s} . Δu and Δd are similarly defined in the following.

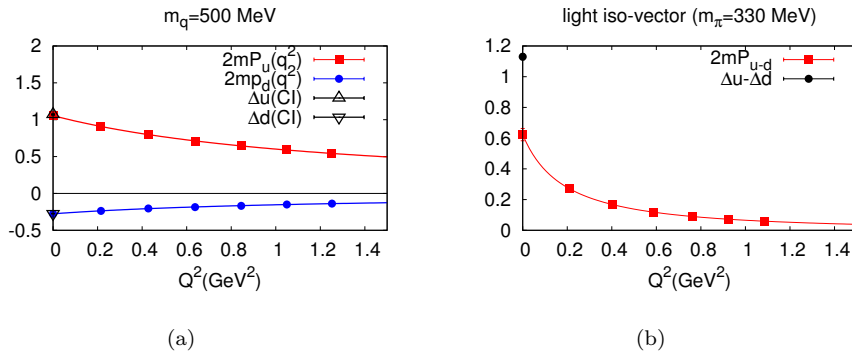


Fig. 4. (a) The quark spin of the proton-like baryon with $m_q \sim 500$ MeV from both the axial vector current and the pseudoscalar term through AWI. In this case, the DI contribution of $2mP$ is canceled by the topological charge term. (b) The same as in (a) for light quarks at the unitary point for isovector g_A^3 which involves only CI.

Since this Δs is quite a bit smaller than the experimental value, we explore the possible finite volume effect and the fact that the induced pseudoscalar form factor $h_A(q^2)$ has been neglected in the Q^2 extrapolation which does not contribute at

the $Q^2 = 0$ limit as in Eq. (16), but has a contribution at finite Q^2 ⁵³. We shall check this in the connected insertion (CI) calculation. As can be seen in Fig. 4 for $m_q \sim 500$ MeV, both Δu and Δd in CI calculated from the axial-vector current and renormalized with Z_A from the isovector Ward identity are well reproduced through the Q^2 extrapolation of $2mP$ with a dipole form. Whereas, in the case of light quarks at the unitary point, $g_A^3 = 1.13(2)$ from the axial-vector current is 1.8(1) times larger than 0.62(4) from the dipole extrapolation of $2mP$. This is most likely due to the ignorance of the induced pseudoscalar form factor $h_A(q^2)$ as well as the finite volume effect at small Q^2 which is well known to plague the Q^2 extrapolation of the nucleon magnetic form factor.

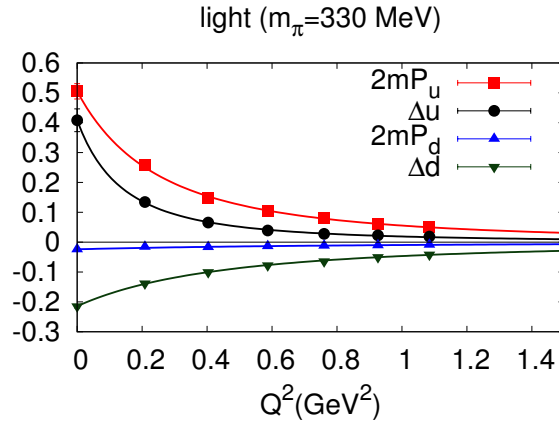


Fig. 5. The combined pseudoscalar contribution from both the connected insertion (CI) and DI ($2mP_{u/d}$ in the plot), along with the overall quark spin from both pseudoscalar and topological charge ($g_{A,d}$). The plot corresponds to the unitary point with $m_\pi = 330$ MeV.

At the unitary point, when the valence u/d mass matches that of the light sea, Fig. 3 shows the quark spin contribution from the combined pseudoscalar terms $2mP_{u/d}$ of the CI and DI with a dipole extrapolation. Also plotted are the overall quark spin $\Delta u/\Delta d$ by including the topological charge contribution. In this case, we obtain $\Delta u + \Delta d = 0.19(3)$ and $\Delta u - \Delta d = 0.62(4)$ at $Q^2 = 0$ from a dipole extrapolation in Q^2 . As we discussed above, the fact that g_A^3 from the axial current is 1.8(1) times larger than that of $\Delta u - \Delta d$ through the Ward identity approach is most likely due to the neglect of the induced pseudoscalar form factor $h_A(q^2)$ and the finite volume effect in the Q^2 extrapolation. We apply this 1.8(1) factor as an estimate to correct the present AWI approach and obtain $\Delta u + \Delta d = 0.35(6)$, $\Delta s = -0.05(1)$. Thus the total estimated spin $\Delta\Sigma = 0.30(6)$ at the unitary point is consistent with the present experimental results which are between 0.2 and 0.3. We expect that, at lighter quark masses, $\Delta\Sigma$ will be smaller.

The above results are from the $24^3 \times 64$ lattice at $m_\pi = 330$ MeV with 200 configurations. The nucleon propagator in the DI has been calculated with the smeared-grid noise source with time dilution which covers all time slices in order to have reasonable statistics for the DI.

4. Glue spin

It has been pointed out that decomposing glue angular momentum into glue spin and orbital angular momentum is only feasible in a specific gauge⁵⁴. Making contact with the parton picture, a spin sum rule involving quark and glue spins and orbital angular momenta is derived in the light-cone gauge (i.e. $A^+ = 0$) with nucleon in the infinite momentum frame⁵⁴. The longitudinal glue spin content is

$$S_G^3 = \langle p, s | \int d^3x \text{Tr}(\vec{E} \times \vec{A})^3 | p, s \rangle / \langle p, s | p, s \rangle, \quad (18)$$

where the nucleon state is in the infinite momentum frame and the gauge potential and the gauge field are in the light-cone gauge. Similarly, a gauge-invariant glue helicity distribution is defined with the light-cone correlation function⁵⁵

$$\Delta g(x) S^+ = \frac{i}{2xP^+} \int \frac{d\xi^-}{2\pi} e^{-ixP^+\xi^-} \langle PS | F_a^{+\alpha}(\xi^-) \mathcal{L}^{ab}(\xi^-, 0) \tilde{F}_{\alpha,b}^+(0) | PS \rangle, \quad (19)$$

where $\tilde{F}^{\alpha\beta} = (1/2) \epsilon^{\alpha\beta\mu\nu} F_{\mu\nu}$ is in the adjoint representation with $\mathcal{A}^+ \equiv T^c A_c^+$, so is the light-cone link $\mathcal{L}(\xi^-, 0) = P \exp[-ig \int_0^{\xi^-} \mathcal{A}^+(\eta^-, 0_\perp) d\eta^-]$.

Since lattice QCD is formulated in Euclidean time, it is not equipped to address the light-cone gauge or the light-cone coordinates and; as such, one is not able to calculate ΔG as defined in Eqs. (18) and (19) on the lattice directly.

On the other hand, a gauge-invariant decomposing of the proton spin has been formulated^{56,57} and examined in various contexts^{58,59,60,61}. It is based on the canonical energy momentum tensor, instead of that in the symmetric Belinfante form. The glue spin operator is

$$\vec{S}_g = \vec{E}^a \times \vec{A}_{phys}^a \quad (20)$$

where $A_{\mu\ phys}$ is the physical component of the gauge field A_μ which is decomposed into $A_{\mu\ phys}$ and a pure gauge part as in QED,

$$A_\mu = A_{\mu\ phys} + A_{\mu\ pure}. \quad (21)$$

They transform homogeneously and inhomogeneously with respect to gauge transformation respectively,

$$\begin{aligned} A_{\mu\ phys} &\rightarrow A'_{\mu\ phys} = g A_{\mu\ phys} g^{-1} \\ A_{\mu\ pure} &\rightarrow A'_{\mu\ pure} = g A_{\mu\ pure} g^{-1} - \frac{i}{g_0} g \partial_\mu g^{-1}, \end{aligned} \quad (22)$$

where g is the gauge transformation matrix and g_0 is the coupling constant. In order to have a unique solution, conditions are set as follows: the pure gauge part does

12 *K.F. Liu*

not give rise to a field tensor by itself and $A_{phys\mu}$ satisfies the non-Abelian Coulomb gauge condition

$$\begin{aligned} F_{\mu\nu pure} &= \partial_\mu A_{\nu pure} - \partial_\nu A_{\mu pure} - ig_0[A_{\mu pure}, A_{\nu pure}] = 0 \\ D_i A_{i phys} &= \partial_i A_{i phys} - ig_0[A_i, A_{i phys}] = 0. \end{aligned} \quad (23)$$

This is analogous to the the situation in QED where the photon spin and orbital angular momentum can be defined^{62,63,64,65} from the canonical energy-momentum tensor

$$\mathbf{S}_A = \int \mathbf{E}_\perp \times \mathbf{A}_\perp d^3x, \quad (24)$$

$$\mathbf{L}_A = \sum_i \int E_i^\perp (\mathbf{x} \times \nabla) A_i^\perp d^3x, \quad (25)$$

where \perp denotes the transverse part. Since they are defined in terms of the transverse parts, they are gauge invariant. However, this gauge invariant definition breaks Lorentz invariance. Nevertheless, it is shown that the ‘spin’ and ‘orbital’ angular momentum so defined are conserved for a free field⁶³. Furthermore, they are observables and can be measured in experiments through interaction with matter. In 1936, Beth had observed one component of the spin angular momentum of light⁶⁶, by measuring the torque on a birefringent plate exerted by a circularly polarized light. Also, it is shown⁶⁷ that the orbital angular momentum of a paraxial laser beam can be measured. Even though gauge invariance is preserved in this canonical formulation, the spin and orbital AM operators are not boost invariant. Since the experiments are conducted in the lab, the formulation is adequate for this single reference frame.

After integrating the longitudinal momentum x , the light-cone operator for the matrix element has the following expression for the glue helicity^{59,68}

$$H_g = \left[\vec{E}^a(0) \times (\vec{A}^a(0) - \frac{1}{\nabla^+} (\vec{\nabla} A^{+,b}) \mathcal{L}^{ba}(\xi^-, 0)) \right]^z \quad (26)$$

It is recently shown⁶⁸ that when boosting the glue spin density operator \vec{S}_g in Eq.(20) to the infinite momentum frame (IMF), the second term in the parentheses on the right side of Eq. (26) is \vec{A}_{pure} . Thus H_g is the glue spin density operator \vec{S}_g in the IMF along the direction of the moving frame. In other words, the longitudinal glue spin operator turns into the helicity operator in the IMF.

To carry out a lattice calculation of the matrix element of the glue spin operator, it is realized⁶⁹ that $A_{\mu phys}$ is related to that fixed in the Coulomb gauge, i.e. $A_{\mu phys} = g_c^{-1} A_c g_c$ where A_c is the gauge potential fixed to the Coulomb gauge and g_c is the gauge transformation that fixes the Coulomb gauge. Since \vec{S}_g is traced over color, the spin operator is then

$$\vec{S}_G = \int d^3x Tr(g_c \vec{E} g_c^{-1} \times \vec{A}_c) = \int d^3x Tr(\vec{E}_c \times \vec{A}_c) \quad (27)$$

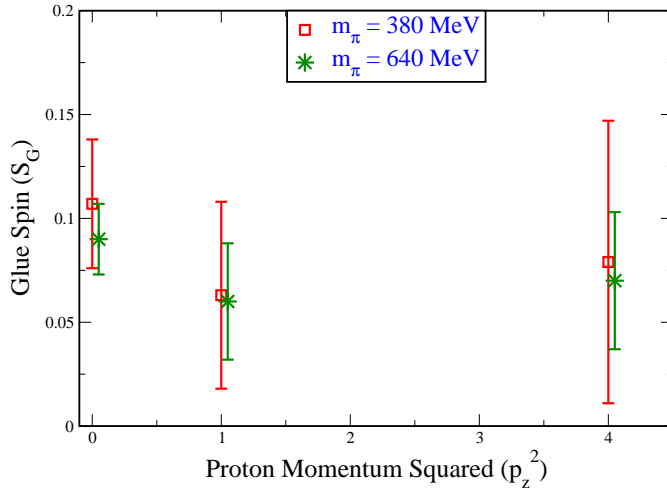


Fig. 6. The results of glue spin S_G in longitudinally polarized proton with longitudinal momenta at 0, 460 MeV and 930 MeV. The quark masses in the nucleon propagator correspond to $m_\pi = 380$ and 640 MeV.

where \vec{E}_c is the electric field in the Coulomb gauge. Although it is gauge invariant since both E and A_{phys} transform homogeneously, it is frame dependent and thus depends on the proton momentum. Its IMF value corresponds to ΔG which is measurable experimentally from high energy proton-proton scattering. The important outcome of the derivation is that glue spin content is amenable to lattice QCD calculation. To the extent that it can be calculated at large enough momentum frame of the proton with enough precision, it can be compared to the experimental glue helicity ΔG .

The first attempt to calculate S_G on the lattice has been carried out on the same set of 2 + 1 flavor dynamical domain-wall configurations on the $24^3 \times 64$ lattice with the sea pion mass at 330 MeV ⁷⁰. The electric field \vec{E} is constructed from the overlap Dirac operator defined in Eq. (7). The gauge potential \vec{A} is obtained from the unsmeared gauge link. We obtained results for the longitudinal nucleon momenta $p_z = n(2\pi/La)$ with $n = 0, 1, 2$ which correspond to 0, 460 MeV and 920 MeV and for the case of quark masses in the nucleon propagator which correspond to $m_\pi = 380$ MeV and 640 MeV. The unrenormalized results are presented in Fig. 6. We see that the preliminary results in Fig. 6 are quite noisy and, as a result, one cannot discern the p_z behavior. The signal can be improved by smearing the link, but it is a challenge to reach large p_z on the lattice. Since one needs p_z to be less than the cutoff, i.e. $p_z a \ll 1$ to avoid large discretization error, this will require a

large lattice size L so that $m_\pi La > 6$ for the nucleon. We note that the question how large a p_z is needed to have the quasi PDFs coincide with the PDFs has been studied in a spectator diquark model ⁷¹. It is found that it is necessary to have p_z as large as 4 GeV for the quasi PDFs to be a good approximation of the PDFs.

5. Summary

We have reported the current lattice efforts in calculating the quark spin, quark orbital angular momentum, glue angular momentum and glue spin in the nucleon. A complete decomposition of the proton momentum and spin into its quark and glue components is given in a quenched approximation. In this case, the glue angular momentum is not further divided into spin and orbital angular momentum parts. The quark spin calculation is recently carried out from the anomalous Ward identity with chiral fermions and is found to be small mainly due to the large negative anomaly term which is believed to be the culprit of the ‘proton spin crisis’. An exploratory lattice calculation of S_G in the non-Abelian Coulomb gauge is carried out ⁷⁰ which has large errors and the nucleon momentum is limited to ~ 1 GeV. The signal of the glue spin S_G can be improved with smearing, but the major challenge is to have a lattice with fine enough lattice spacing to accommodate large momentum states and show that the infinite momentum extrapolation can be made under control.

Acknowledgments

This work is partially supported by USDOE grant DE-FG05-84ER40154. The author would like to thank X.S. Chen, X. Ji, L. Gamberg, Y. Hatta, E. Leader, C. Lorcé, M. Wakamatsu, and Y. Zhao for helpful and insightful discussions. He also thanks E. Leader and D. Stamenov for providing the strange quark spin contribution from their analysis.

References

1. D. de Florian, R. Sassot, M. Stratmann and W. Vogelsang, Phys. Rev. D **80**, 034030 (2009) [arXiv:0904.3821 [hep-ph]].
2. S. J. Dong, J. -F. Lagae, K. F. Liu, Phys. Rev. Lett. **75**, 2096-2099 (1995), [hep-ph/9502334].
3. M. Fukugita, Y. Kuramashi, M. Okawa and A. Ukawa, Phys. Rev. Lett. **75**, 2092 (1995), [hep-lat/9501010].
4. S. Gusken *et al.* [TXL Collaboration], Phys. Rev. D **59**, 114502 (1999).
5. G. S. Bali *et al.* [QCDSF Collaboration], Phys. Rev. Lett. **108**, 222001 (2012), [arXiv:1112.3354 [hep-lat]].
6. M. Engelhardt, Phys. Rev. D **86**, 114510 (2012) [arXiv:1210.0025 [hep-lat]].
7. A. Abdel-Rehim, C. Alexandrou, M. Constantinou, V. Drach, K. Hadjiyiannakou, K. Jansen, G. Koutsou and A. Vaquero, arXiv:1310.6339 [hep-lat].
8. R. Babich, R. C. Brower, M. A. Clark, G. T. Fleming, J. C. Osborn, C. Rebbi and D. Schaich, Phys. Rev. D **85**, 054510 (2012) [arXiv:1012.0562 [hep-lat]].

9. E. Leader, A. V. Sidorov and D. B. Stamenov, *Phys. Rev. D* **91**, no. 5, 054017 (2015) [arXiv:1410.1657 [hep-ph]].
10. E. Leader and D. B. Stamenov, private communication.
11. Y. B. Yang, M. Gong, K. F. Liu and M. Sun, *PoS LATTICE* **2014**, 138 (2014) [arXiv:1504.04052 [hep-ph]].
12. N. Mathur, S. J. Dong, K. F. Liu, L. Mankiewicz, N. C. Mukhopadhyay, *Phys. Rev. D* **62**, 114504 (2000), [hep-ph/9912289].
13. P. Hagler *et al.* [LHPC and SESAM Collaborations], *Phys. Rev. D* **68**, 034505 (2003), [hep-lat/0304018].
14. M. Gockeler *et al.* [QCDSF Collaboration], *Phys. Rev. Lett.* **92**, 042002 (2004) [hep-ph/0304249].
15. D. Brommel *et al.* [QCDSF-UKQCD Collaboration], *PoS LATTICE* **2007**, 158 (2007), [arXiv:0710.1534 [hep-lat]].
16. J. D. Bratt *et al.* [LHPC Collaboration], *Phys. Rev. D* **82**, 094502 (2010) [arXiv:1001.3620 [hep-lat]].
17. C. Alexandrou, J. Carbonell, M. Constantinou, P. A. Harraud, P. Guichon, K. Jansen, C. Kallidonis and T. Korzec *et al.*, *Phys. Rev. D* **83**, 114513 (2011) [arXiv:1104.1600 [hep-lat]].
18. S. N. Syritsyn, J. R. Green, J. W. Negele, A. V. Pochinsky, M. Engelhardt, P. Hagler, B. Musch and W. Schroers, *PoS LATTICE* **2011** (2011) 178 [arXiv:1111.0718 [hep-lat]].
19. C. Alexandrou, M. Constantinou, S. Dinter, V. Drach, K. Jansen, C. Kallidonis and G. Koutsou, *Phys. Rev. D* **88**, 014509 (2013) [arXiv:1303.5979 [hep-lat]].
20. C. Adolph *et al.* [COMPASS Collaboration], *Phys. Rev. D* **87**, 052018 (2013); [arXiv:1211.6849 [hep-ex]]; C. Adolph *et al.* [COMPASS Collaboration], *Phys. Lett. B* **718**, 922 (2013) [arXiv:1202.4064 [hep-ex]].
21. P. Djawotho [STAR Collaboration], *J. Phys. Conf. Ser.* **295**, 012061 (2011).
22. A. Airapetian *et al.* [HERMES Collaboration], *JHEP* **1008**, 130 (2010) [arXiv:1002.3921 [hep-ex]].
23. M. Stolarski [COMPASS Collaboration], *Nucl. Phys. Proc. Suppl.* **207-208**, 53 (2010).
24. A. Adare *et al.* [PHENIX Collaboration], *Phys. Rev. D* **79**, 012003 (2009) [arXiv:0810.0701 [hep-ex]].
25. E. C. Aschenauer, A. Bazilevsky, K. Boyle, K. O. Eysler, R. Fatemi, C. Gagliardi, M. Grosse-Perdekamp and J. Lajoie *et al.*, arXiv:1304.0079 [nucl-ex].
26. M. G. Alekseev *et al.* [COMPASS Collaboration], *Phys. Lett. B* **690**, 466 (2010) [arXiv:1001.4654 [hep-ex]]; *Phys. Lett. B* **693**, 227 (2010) [arXiv:1007.4061 [hep-ex]].
27. D. de Florian, R. Sassot, M. Stratmann and W. Vogelsang, *Phys. Rev. Lett.* **113**, no. 1, 012001 (2014) [arXiv:1404.4293 [hep-ph]].
28. L. Adamczyk *et al.* [STAR Collaboration], arXiv:1405.5134 [hep-ex].
29. A. Adare *et al.* [PHENIX Collaboration], *Phys. Rev. D* **90**, no. 1, 012007 (2014) [arXiv:1402.6296 [hep-ex]].
30. S. J. Brodsky and S. Gardner, *Phys. Lett. B* **643**, 22 (2006) [hep-ph/0608219].
31. K. F. Liu, M. Deka, T. Doi, Y. B. Yang, B. Chakraborty, Y. Chen, S. J. Dong and T. Draper *et al.*, *PoS LATTICE* **2011** (2011) 164 [arXiv:1203.6388 [hep-ph]].
32. M. Deka, T. Doi, Y. B. Yang, B. Chakraborty, S. J. Dong, T. Draper, M. Glatzmaier, M. Gong, H.W. Lin, K.F. Liu, D. Mankame, N. Mathur, and T. Streuer, *Phys. Rev. D* **91**, no. 1, 014505 (2015) [arXiv:1312.4816 [hep-lat]].
33. X. D. Ji, *Phys. Rev. Lett.* **78**, 610 (1997) [hep-ph/9603249].
34. W. Wilcox, *Phys. Rev. D* **66**, 017502 (2002) [hep-lat/0204024].
35. K. F. Liu, A. Alexandrou and I. Horvath, *Phys. Lett. B* **659**, 773 (2008) [hep-lat/0703010 [HEP-LAT]].

16 *K.F. Liu*

36. A. Alexandru, I. Horvath and K. F. Liu, Phys. Rev. D **78**, 085002 (2008) [arXiv:0803.2744 [hep-lat]].
37. O. V. Teryaev, hep-ph/9904376.
38. S. J. Brodsky, D. S. Hwang, B. -Q. Ma and I. Schmidt, Nucl. Phys. B **593**, 311 (2001) [hep-th/0003082].
39. M. Glatzmaier and K. F. Liu, arXiv:1403.7211 [hep-lat].
40. K. F. Liu, S. J. Dong, Phys. Rev. Lett. **72**, 1790-1793 (1994), [hep-ph/9306299].
41. K. F. Liu, S. J. Dong, T. Draper, D. Leinweber, J. H. Sloan, W. Wilcox, R. M. Woloshyn, Phys. Rev. **D59**, 112001 (1999), [hep-ph/9806491].
42. K. F. Liu, Phys. Rev. **D62**, 074501 (2000), [hep-ph/9910306].
43. K. -F. Liu, W. -C. Chang, H. -Y. Cheng and J. -C. Peng, Phys. Rev. Lett. **109**, 252002 (2012) [arXiv:1206.4339 [hep-ph]].
44. L. H. Karsten and J. Smit, Nucl. Phys. B **183**, 103 (1981).
45. J. F. Lagae and K. F. Liu, Phys. Rev. D **52**, 4042 (1995) [hep-lat/9501007].
46. H. Neuberger, Phys. Lett. B **417**, 141 (1998) [hep-lat/9707022].
47. M. Luscher, Phys. Lett. B **428**, 342 (1998) [hep-lat/9802011].
48. P. Hasenfratz, V. Laliena and F. Niedermayer, Phys. Lett. B **427**, 125 (1998) [hep-lat/9801021].
49. Y. Kikukawa and A. Yamada, Phys. Lett. B **448**, 265 (1999) [hep-lat/9806013]; D. H. Adams, Annals Phys. **296**, 131 (2002) [hep-lat/9812003]; K. Fujikawa, Nucl. Phys. B **546**, 480 (1999) [hep-th/9811235]; H. Suzuki, Prog. Theor. Phys. **102**, 141 (1999) [hep-th/9812019].
50. Y. Kikukawa and A. Yamada, Nucl. Phys. B **547**, 413 (1999) [hep-lat/9808026].
51. M. Gong *et al.* [XQCD Collaboration], Phys. Rev. D **88**, no. 1, 014503 (2013) [arXiv:1304.1194 [hep-ph]].
52. M. Franz, M. V. Polyakov and K. Goeke, Phys. Rev. D **62**, 074024 (2000) [hep-ph/0002240].
53. K. F. Liu, hep-lat/9510046; K. F. Liu, S. J. Dong, T. Draper and W. Wilcox, Phys. Rev. Lett. **74**, 2172 (1995) [hep-lat/9406007].
54. R. L. Jaffe and A. Manohar, Nucl. Phys. B **337**, 509 (1990).
55. A. V. Manohar, Phys. Rev. Lett. **65**, 2511 (1990)
56. X. -S. Chen, X. -F. Lu, W. -M. Sun, F. Wang and T. Goldman, Phys. Rev. Lett. **100**, 232002 (2008) [arXiv:0806.3166 [hep-ph]].
57. X. -S. Chen, W. -M. Sun, X. -F. Lu, F. Wang and T. Goldman, Phys. Rev. Lett. **103**, 062001 (2009) [arXiv:0904.0321 [hep-ph]].
58. M. Wakamatsu, Phys. Rev. D **81**, 114010 (2010) [arXiv:1004.0268 [hep-ph]].
59. Y. Hatta, Phys. Rev. D **84**, 041701 (2011) [arXiv:1101.5989 [hep-ph]].
60. Y. M. Cho, M. -L. Ge and P. Zhang, Mod. Phys. Lett. A **27**, 1230032 (2012) [arXiv:1010.1080 [nucl-th]].
61. E. Leader and C. Lorc, Phys. Rept. **541**, 163 (2014) [arXiv:1309.4235 [hep-ph]].
62. C. Cohen-Tannoudji, J. Dupont-Roc, and G. Grynberg, Photons and Atoms (Wiley, New York 1989).
63. S.J. van Enk and G. Nienhuis, J. Mod. Opt. **41**, 963 (1994); S.J. van Enk and G. Nienhuis, Europhys. Lett. **25**, 497 (1994).
64. K. Y. Bliokh, A. Y. Bekshaev and F. Nori, New J. Phys. **15**, 033026 (2013) [arXiv:1208.4523 [physics.optics]]; *ibid* 073022 (2013).
65. K. Y. Bliokh, J. Dressel and F. Nori, New J. Phys. **16**, no. 9, 093037 (2014) [arXiv:1404.5486 [physics.optics]].
66. R.A. Beth, Phys. Rev. **50**, 115 (1936).
67. L. Allen, M.W. Beijersbergen, R.J.C. Spreeuw, and J.P. Woerdman, Phys. Rev. **A**

- 45**, 8185 (1992); S.J. van Enk and G. Nienhuis, *Opt. Commun.* **94**, 147 (1992); M.W. Beijersbergen, L. Allen, H.E.L.O. van der Veen, and J.P. Woerdman, *Opt. Commun.* **96**, 123 (1993).
68. X. Ji, J. H. Zhang and Y. Zhao, *Phys. Rev. Lett.* **111**, 112002 (2013) [arXiv:1304.6708 [hep-ph]].
69. Y.B. Yang and K.F. Liu, under preparation.
70. R. S. Sufian, M. J. Glatzmaier, Y. B. Yang, K. F. Liu and M. Sun, arXiv:1412.7168 [hep-lat].
71. L. Gamberg, Z. B. Kang, I. Vitev and H. Xing, *Phys. Lett. B* **743**, 112 (2015) [arXiv:1412.3401 [hep-ph]].